

Systematic identification of disease-causing promoter and untranslated region variants in 8,040 undiagnosed individuals with rare disease

Alexandra C Martin-Geary^{1,2}, Alexander J M Blakes³, Ruebena Dawes^{1,2}, Scott D Findlay⁴, Jenny Lord⁵, Susan Walker⁵, Jonathan Talbot-Martin⁷, Nechama Wieder^{1,2}, Elston N D'Souza^{1,2}, Maria Fernandes^{1,2}, Sarah Hilton⁸, Nayana Lahiri⁹, Christopher Campbell⁸, Sarah Jenkinson⁸, Christian G E L DeGoede^{10,11}, Emily R Anderson¹², Christopher B. Burge⁴, Stephan J Sanders^{13,14,15}, Jamie Ellingford^{3,8}, Diana Baralle⁶, Siddharth Banka⁸, and Nicola Whiffin^{1,2,16}

1. Big Data Institute, University of Oxford, UK
2. Wellcome Centre for Human Genetics, University of Oxford, UK
3. Manchester Centre for Genomic Medicine, Division of Evolution and Genomic Sciences, School of Biological Sciences, Faculty of Biology, Medicine and Health, University of Manchester, Manchester, UK
4. Department of Biology, Massachusetts Institute of Technology, Cambridge, USA
5. Genomics England, UK
6. School of Human Development and Health, Faculty of Medicine, University of Southampton, Southampton, United Kingdom
7. Department of Bioengineering, Imperial College London, UK
8. Manchester Centre for Genomic Medicine, Manchester University NHS Foundation Trust, Health Innovation Manchester, Manchester M13 9WL, UK
9. St George's, University of London & St George's University Hospitals NHS Foundation Trust, Institute of Molecular and Clinical Sciences, London, SW17 0QT, UK
10. Department of Paediatric Neurology, Clinical research Facility, Lancashire Teaching Hospitals NHS Trust
11. Manchester Metropolitan University
12. Liverpool Centre for Genomic Medicine, Liverpool Women's Hospital, Liverpool, UK

NOTE: This preprint reports new research that has not been certified by peer review and should not be used to guide clinical practice.

13. Institute of Developmental and Regenerative Medicine, Department of Paediatrics, University of Oxford, Oxford, OX3 7TY, UK
14. Department of Psychiatry and Behavioral Sciences, UCSF Weill Institute for Neurosciences, University of California, San Francisco, San Francisco, CA 94158, USA
15. New York Genome Center, New York, NY, USA
16. Program in Medical and Population Genetics, Broad Institute of MIT and Harvard, Cambridge, MA, USA

Correspondence should be addressed to Alexandra Martin-Geary (alex.geary@well.ox.ac.uk) or Nicola Whiffin (nwhiffin@well.ox.ac.uk)

Abstract

Background

Both promoters and untranslated regions (UTRs) have critical regulatory roles, yet variants in these regions are largely excluded from clinical genetic testing due to difficulty in interpreting pathogenicity. The extent to which these regions may harbour diagnoses for individuals with rare disease is currently unknown.

Methods

We present a framework for the identification and annotation of potentially deleterious proximal promoter and UTR variants in known dominant disease genes. We use this framework to annotate *de novo* variants (DNVs) in 8,040 undiagnosed individuals in the Genomics England 100,000 genomes project, which were subject to strict region-based filtering, clinical review, and validation studies where possible. In addition, we performed region and variant annotation-based burden testing in 7,862 unrelated probands against matched unaffected controls.

Results

We prioritised eleven DNVs and identified an additional variant overlapping one of the eleven. Ten of these twelve variants (82%) are in genes that are a strong match to the individual's phenotype and six had not previously been identified. Through burden testing, we did not observe a significant enrichment of potentially deleterious promoter and/or UTR variants in individuals with rare disease collectively across any of our region or variant annotations.

Conclusions

Overall, we demonstrate the value of screening promoters and UTRs to uncover additional diagnoses for previously undiagnosed individuals with rare disease and provide a framework for doing so without dramatically increasing interpretation burden.

Keywords

Untranslated regions, promoters, splicing, rare disease, non-coding, regulatory regions

Background

Current approaches to identify a genetic diagnosis for individuals with rare disease are heavily focussed on protein-coding regions of the genome. Even where genome sequencing data are available, analysis methods often exclude variants that are not in, or immediately adjacent to protein-coding exons. This is in large part due to the difficulty in interpreting variants outside of these regions, but also due to the increased burden of variant review in a clinical context. Studies that have investigated a wider genomic context have successfully identified variants in non-coding regions that cause penetrant Mendelian disease(1–3). The majority of these studies have, however, focussed on small numbers of individuals, specific phenotypes, and/or limited genetic regions. Consequently, we still do not know what

proportion of currently genetically undiagnosed individuals with rare disease carry disease-causing variants in non-coding regions.

In this work, we focus on promoters and untranslated regions (UTRs) given that these regions can be confidently linked to known disease genes, and variants within them can significantly disrupt normal gene regulation and have previously been implicated in rare disease(4,5). In short, they provide the best opportunity to expand clinical screening into non-coding regions.

UTRs are regulatory sequences encoded immediately up- and down-stream of the coding sequence (CDS) of protein-coding genes. These regions have important roles in regulating RNA stability, RNA localisation, and the rate of CDS translation(6,7). Variants in UTRs that disrupt these regulatory processes have been shown to cause rare disease through a variety of mechanisms(8). For example, 5'UTR variants that disrupt translation by creating upstream start codons (uAUGs) or perturbing upstream open reading frames (uORFs) cause a range of phenotypes including in genes causing severe developmental disorders (e.g. *NF1*(9) and *MEF2C*(2), whilst variants directly upstream of the CDS in the *GATA4* gene, that alter the 'Kozak' consensus (i.e., the AUG start codon and surrounding motif) have been linked to atrial septal defect(10). Variants resulting in aberrant splicing of the *PAX6* 5'UTR are a frequent cause of aniridia(11). 3'UTR variants that disrupt polyadenylation signals or RNA Binding protein (RBP) binding sites in the α and β -globin genes have been found in individuals with α and β -thalassemia(12). A comprehensive search for 5'UTR variants in retinal disease patients uncovered variants that cause disease through a variety of mechanisms(13).

Proximal promoters comprise an open region of chromatin spanning both up- and down-stream of the transcription start site (TSS) to which transcription factors and polymerase bind to initiate transcription. Variants within promoter regions that disrupt

transcription by altering transcription factor binding, or by changing methylation patterns have been identified as being causal of a number of diseases, including *TERT* promoter variants in idiopathic pulmonary fibrosis(14) and *CAMK1D* promoter variants in type 2 diabetes(15). Whilst there are many documented mechanisms through which UTR and promoter variants cause rare phenotypes, our knowledge is likely far from complete. It is also unclear to what extent increasing our understanding of, and regularly including these regions in clinical testing pipelines, will uncover novel diagnoses for currently undiagnosed individuals with rare disorders.

Here, we used the Genomics England 100,000 Genomes Project (GEL) dataset to systematically identify and annotate variants in promoters, UTRs, and UTR introns in 8,040 undiagnosed trios. We developed a reproducible annotation approach with high specificity that can be used in clinical settings without dramatically increasing the number of candidate variants for manual review. After employing strict region-based filters we identified ten likely diagnostic variants, nine *de novo* and one additional overlapping variant. Comparing individuals with rare disorders to matched controls we did not identify a significant burden of rare potentially disruptive variants collectively across any region type or variant annotation, although this may be due to limited statistical power. Our results highlight how promoter and UTR regions can be effectively searched for new diagnoses in rare disease patients and we outline a framework for identification and annotation of such variants in large-scale cohorts.

Methods

Identifying known disease genes using PanelApp

PanelApp gene panels were obtained from panelapp.genomicsengland.co.uk using lynx v2.8.9(16), on 12/09/2022. These were filtered to include only the 6,504 genes where the

strength of association for one or more gene panel was “green”, corresponding to those with a confident link to the phenotype.

We further filtered to only include genes known to cause a disorder with a dominant mode of inheritance (MOI), inclusive of any genes associated with both dominant and recessive phenotypes. Finally, we selected only genes with transcripts in the MANE v1.0 dataset (17). In total we included 1,536 genes/1,567 transcripts.

Annotating non-coding regions of interest

Transcripts were defined using MANE v1.0, inclusive of 19,062 MANE ‘select’ and 58 ‘plus clinical’ transcripts(17). UTR exon and intron coordinates were taken directly from the MANE .gff file.

Proximal promoter regions were defined using candidate *cis* regulatory elements (cCREs) obtained from ENCODE(18). Accurate promoter definition is hampered by their tissue specificity. In tissues where a promoter is inactive, it is often marked by a minimal nucleosome free region, but this region may be expanded when the promoter is active. To account for this, as well as promoters that are not annotated at all in the ENCODE dataset, we calculated the average size of all ‘promoter-like’ cCREs that overlap with TSS of MANE transcripts. We calculated the 25th and 75th percentiles of the distribution of distances these cCREs extend up- (25%=181bp; 75%=266bp) and down-stream (25%=67bp; 75%=139bp) of the TSS (Supplementary Figure 1). The 25th percentiles (-181bp to +67bp from TSS) were used to define a ‘minimal’ promoter region.

For transcripts with a cCRE that overlaps the TSS:

- If the cCRE extends ≥ 181 bp upstream and ≥ 67 bp downstream of the TSS (i.e. at least the minimal 25th percentile definition) the exact region defined by the cCRE is used (Supplementary Figure 1d; n=7,368).
- If the cCRE falls short in either (or both) direction(s), it is extended to reach the 25th percentile distance in that/those direction(s) (Supplementary Figure 1e; extended upstream n=2,953; extended downstream n=2,918, extended in both directions n=464).

For transcripts with no TSS overlapping cCRE (n=5,417), the 75th percentiles are used to define a promoter region that stretches 266bp up- and 139bp down-stream of the TSS.

To ensure identified variants don't have a protein-coding impact(19) we used bedtools(19) to exclude any positions that intersect with a CDS position in any MANE transcript. In total, we defined 20,417,669 near-coding bases across the 1,567 green PanelApp genes, for an average of 13,030 bases per transcript (min=264, max=791,387), and between 17 and 18,786 per region (Supplementary Table 1). The final set of near-coding regions defined across all green PanelApp genes is in Supplementary Table 2.

Identifying and filtering *de novo* variants

We used a dataset of previously identified and filtered *de novo* variants (DNVs) within GEL(20), accessed using the RLabKey API(21). We filtered individuals to remove any with subsequently withdrawn consent, and to only include those with a 'participant type' of 'proband', where neither parent was classified as 'affected' or had any associated Human Phenotype Ontology (HPO) terms, and for whom variant calls were on the GRCh38 reference genome. This resulted in an initial set of 9,665 trio probands.

Variants were filtered to only those that passed the most stringent set of GEL filters(22). We removed variants with allele frequency (AF) ≥ 0.00005 and allele count (AC) ≥ 5 in the GEL defined set of 55,603 unrelated individuals or with AF ≥ 0.0005 in any of the major population groups in gnomAD v3.1.1.(23). We restricted our analyses to DNVs within our defined near-coding regions of PanelApp genes with high confidence phenotypic associations (flagged as ‘green’ genes) for the individual’s phenotype. Finally, we excluded participants with an identified coding diagnosis (see below). This resulted in a set of 1,278 DNVs, in 1,094 probands.

Identifying individuals with existing diagnoses

A list of all participants for whom a confirmed diagnosis was recorded was obtained from the Genomics England ‘exit questionnaire’ table, identified with those for whom the family case was flagged as “solved”. The associated variants were cross referenced with MANE v1.0 coding regions and our promoter, UTR, and UTR intronic regions, with variants mapped onto GRCh38 by the ‘LiftOver’(24) tool, where required.

Region level variant annotations

Variants for both the *de novo* and burden testing arms of our analysis underwent initial annotation using Ensembl’s variant effect predictor (VEP) v99.1(25) with UTRannotator, SpliceAI v1.3, and CADD v.1.6 plugins(26), as well as custom annotations for PhyloP 100 way vertebrate conservation scores(27), and ClinVar (28) clinical significance annotations (accessed 2022/08/12).

5’UTR variants annotated by UTRannotator(29) were filtered to identify those with the highest likelihood of disrupting translation. To this end, we extracted all variants annotated as:

- uAUG gain resulting in creation of an overlapping open reading frame (oORF) with a strong or moderate Kozak consensus sequence;
- uSTOP loss, with no alternate stop prior to the CDS start (i.e. also resulting in an oORF) and a strong or moderate Kozak consensus sequence;
- uAUG loss, with strong Kozak consensus sequence;
- uFrameshift resulting in an oORF with a strong or moderate Kozak consensus sequence.

For SpliceAI scores, we took the highest delta value across all predictions, with a cutoff of 0.2 for the *de novo* analysis and 0.5 for the burden testing.

Variants across all regions with a ClinVar annotation indicating a benign or protective effect (benign, likely benign, benign/likely benign, protective) were excluded.

Cut-offs for CADD PHRED(26) (25.3) and PhyloP(27) (7.367) scores were taken as the supporting evidence thresholds from Pejaver *et al*(30). For variants with multiple recorded scores, the maximum was taken. We note that these scores were calibrated for missense variants, but no alternative exists for non-coding region variants due to the paucity of variants available to benchmark against. Due to this, CADD PHRED and PhyloP scores were not used to annotate variants in deep intronic regions (>20bp from the end of the exon), to reduce noise.

Internal ribosome entry site (IRES) data were obtained from IRESbase(31) on 23/08/2022, microRNA (miRNA) binding sites were obtained from the literature(32–35), and downstream open reading frame (dORF) coordinates were obtained from Chothani *et al*(36). For each, locations were cross referenced with our variant positions, and any intersecting variant flagged.

Given the large proportion of variants that fall into miRNA and IRES sites, we excluded any variants that also had a CADD ≤ 22.7 or PhyloP ≤ 1.879 . These scores were suggested by Pejaver *et al* as supporting evidence for a benign classification(30).

Kozak consensus sequence variants in the -3 position were identified with reference to MANE v1.0 CDS start positions (i.e. the R of the gccRccAUGG motif). Any variant that changed a reference A or G to a C or T was annotated as potentially Kozak disrupting(37).

RNA binding protein predictions were generated using the methods detailed in Findlay *et al*(38) for all possible variants within motifs that are proximal to ENCODE eCLIP sites, that are also high affinity sites as predicted by RBPamp(39). These were intersected with our variants and filtered to retain only those with a reference affinity of ≥ 0.1 and with an impact of 'loss of binding' predicted by the RBP binding affinity model (defined as alternative allele affinity / reference allele affinity $< 1/3$).

Using MANE v1.0 mRNA sequences, we identified the locations of all 3'UTR AAUAAA and AUUAAA polyA signal motifs. We filtered intersecting variants to those that did not result in the creation of an alternative known motif (AAUAAA, AUUAAA, AGUAAA, UAUAAA, CAUAAA, GAUAAA, AAUAUA, AAUACA, AAUAGA, AAAAAG, ACUAAA, or AAAAAA)(40).

Transcription factor binding site (TFBS) locations were obtained from ENCODE(41) and converted using bigBedToBed(24) on the command line, resulting in 4,465,728 TFBS footprints. Any variant not within a footprint identified by ENCODE as falling within the 'core' region of a DNase I hypersensitive (DHS) peak was excluded. Remaining variants were annotated using FABIAN(42), limiting to only transcription factor flexible models as these have been shown to outperform positional weight matrices(43). The resultant data was transformed to produce one score per transcription factor, per variant:

$$Score = (\sum AI:AN)/N$$

Where A is each model's predicted change in binding affinity and ' N ' is the total number of these predictions provided for that transcription factor. Scores ≥ 0.04 were recorded as predicted gain and those ≤ -0.04 as predicted loss. For each variant we then calculated the mean gain/loss/total scores and retained any variant with a loss score ≤ -0.4 .

Clinical Review of candidate variants

For each participant carrying a candidate diagnostic *de novo* variant, we compared the similarity between the HPO terms assigned at recruitment with the phenotype expected for a heterozygous loss of function variant in the gene. Variants were interpreted under the assumption that they caused loss-of-function (LoF) and were of high penetrance. Expected phenotypes for each gene were sought from OMIM and the published literature. Where we identified a plausible phenotype match, we raised a clinical collaboration request with Genomics England to confirm or refute our findings by collaboration with the recruiting clinician.

Defining case and control sets for burden testing

From GEL version 15, we selected participants meeting all of the following criteria:

1. Variants called on genome build 'GRCh38 and with delivery version 'V4'
2. Consent not subsequently withdrawn
3. Karyotype one of 'XX', 'XY', 'NA', 'Other' and karyotypic and phenotypic sex not in conflict

Cases were defined as:

1. Individuals with a participant type of 'proband'
2. With at least one 'green' PanelApp gene in a virtual gene panel assigned to them
3. Without an existing coding diagnosis (see above).

Controls were taken as the unaffected parents of participants with rare disease. Defined as:

1. Participant type is 'Mother' or 'Father'
2. Affected status is 'Unaffected'
3. No recorded HPO terms

The genetically-inferred ancestry of each participant, as calculated by GEL, was obtained from LabKey. Participants with a single origin ancestry match of 99% or greater were retained and defined as that ancestry(44). Through this approach, we defined a total of 19,220 cases and 20,683 controls.

Filtering aggregated variants

Variants within MANEv1.0 transcripts, for all potential case and control participants that passed all internal QC filters were extracted from the aggregated variant VCF files in GEL(45).

In line with recommendations from Pedersen *et al*(46) we filtered variants to those with genotype quality (GQ) ≥ 20 , read depth (DP) ≥ 10 , missingness $\leq 5\%$ heterozygous allele balance (AB) $0.2 \leq AB \leq 0.8$, and homozygous AB ≤ 0.02 . If a variant call failed one or more of these filters in 25% or more cases that call was excluded. We further filtered to only those with GEL internal and gnomAD (v3.1.1; in any population) AF ≤ 0.0001 . We retained a total of 18,498,584 variants, a mean variant count per individual of 463.59 (461.74 in cases and 465.74 in controls).

Participant Matching

To exclude any individuals with very high numbers of called variants (suggestive of systematic error), we calculated a population-specific Z-score per participant as follows:

$$z = (x - \mu) / \sigma$$

Where 'x' is the variant count in that participant, across all MANE transcripts, from the start of the promoter to the transcript end, ' μ ' is the population mean, and ' σ ' is the population standard deviation, where the population is all individuals defined of the same genetic ancestry (see above). Participants with a Z-score of ± 2 were dropped (N=1,560, 728 probands, 832 controls) resulting in a set of 18,492 probands and 19,851 control participants.

Within each cohort, we removed individuals with KING score(47) ≥ 0.0442 within the Genomics England relatedness data(44), indicative of being a 3rd degree relative, by randomly selecting one participant for removal in an iterative process until no further relatedness in individuals was detected.

We then matched each proband 1:1 with a single control participant by sex and genetically-inferred ancestry, ensuring that the matched proband and control did not share a family ID. The resultant matched cohort consisted of 18,304 probands, paired with 11,641 unique controls. To avoid potential biases when matching participants caused by low population numbers, we limited to genetically-inferred ancestries where the number of both case and control participants was > 200 . This resulted in a cohort of 17,641 case probands, and 11,227 control participants with either European or South Asian genetically-inferred ancestry (Supplementary Table 3). To limit bias due to the presence of large gene panels, this cohort was then limited to probands who had 100 or fewer green dominant genes assigned (Supplementary Figure 2), resulting in a final cohort of 7,862 probands and 6,371 matched controls.

Burden testing

Aggregated variants filtered as above were further restricted to those with $AF \leq 0.00005$ for both internal and gnomAD major population frequencies and to exclude any with an allele count (AC) across the entirety of AggV2 of ≥ 5 . These 1,079,616 variants were annotated and filtered with reference to the annotations described above, with the addition of a more stringent SpliceAI threshold of 0.5 (Supplementary Figure 3).

A simple burden test was performed across all defined near-coding region and variant annotations comparing individuals that had one or more annotated variants meeting our criteria in any near coding region to those that did not, using a Fisher's exact test performed in R (Supplementary Table 3). The test was repeated for each region annotation separately, using Bonferroni correction for multiple testing.

To estimate the number of participants required to see a significant enrichment across all region and variant annotations, we iteratively increased the number of case and control participants by 1, while maintaining the proportion of observed cases and controls with candidate variants. Fisher's tests were performed for each iteration, until the resulting P -value was ≤ 0.0031 , a Bonferroni adjusted threshold accounting for 16 tests.

RNA sequencing

Blood was collected from a subset of 100,000 Genomes Project probands in PaxGene tubes to preserve RNA at the time of recruitment. RNA was extracted, depleted of globin and ribosomal RNAs, and subjected to sequencing by Illumina using 100bp paired-end reads, with a mean of 102M mapped reads per individual. Alignment was performed using Illumina's DRAGEN pipeline. IGV(48) was used to inspect sequencing reads and generate Sashimi plots to show splicing junctions supported by 5 or more reads in areas of interest.

FRASER2(49) and OUTRIDER(50) were used to detect abnormal splicing events and expression differences with 499 samples used as controls.

DNA methylation analyses

DNA methylation array testing was performed on a diagnostic basis as described previously(51,52).

Availability of data and materials

The datasets supporting the conclusions of this article are available in the near-coding annotation github repository

(https://github.com/Computational-Rare-Disease-Genomics-WHG/Near_coding_annotation).

Unless otherwise stated, all analyses were performed using R Statistical software version 4.0.2(53), with the packages 'dplyr'(54), 'tidyr'(55), 'stringr'(56), 'Rlabkey'(21), 'UpSetR'(57), and 'ggplot2'(58).

Results

Strict region-specific filtering prioritises likely deleterious de novo promoter and UTR variants

We identified 767,063 rare ($AF \leq 0.005\%$) high-confidence DNVs in 10,665 trio probands in GEL (71.9 per proband), 685,438 of these variants were in participants whose parents were classed as unaffected and had no HPO terms (9,665 probands). Of the remaining probands, 8,040 did not have an existing confirmed diagnosis attributed to a coding variant (576,030 variants, 71.6 per proband). We filtered to include only DNVs in UTR exons and introns (both defined using MANEv1.0 transcripts), and promoter regions (defined by ENCODE candidate

cis regulatory elements; see Methods). Henceforth, we collectively refer to these regions as ‘near-coding’. We limited our analysis to variants which fell in or near known monogenic disorder genes (3,316 variants) and filtered these to genes which could be plausibly associated with the participant’s phenotype. Accordingly, we filtered for DNVs of genes flagged as ‘green’ in one or more PanelApp(59) gene panel(s) assigned to the individual, and which were associated with disorders with a dominant mode of inheritance. Of note, 309 probands did not have any assigned green dominant genes. In total, we proceeded with 1,311 candidate DNVs in 1,118 probands.

To identify likely disease-causing DNVs we used a region-specific annotation and filtering approach. We prioritised 5’UTR variants that create uAUGs or disrupt uORFs using UTRannotator(29), that overlap *IRES* defined by IRESbase(31), or that lead to disruption of the Kozak consensus sequence(37). 3’UTR variants were prioritised if they disrupt a polyadenylation site or signal sequence, disrupt a miRNA binding site, disrupt an RBP motif, or if they disrupt the start/stop of a dORF with evidence of translation from ribosome profiling (from Chothani *et al*(36)). Given the large numbers of variants annotated as within IRES or miRNA binding sites, these variants were further filtered to remove any with CADD (<22.7) or PhyloP (<1.879) scores in support of being benign(30). Across all UTR exons, and in 5’ and 3’ UTR introns, variants with SpliceAI masked delta scores ≥ 0.2 were prioritised. Promoter variants were prioritised if they are predicted to disrupt a transcription factor binding site using FABIAN(42). Finally, across all region annotations, variants with a CADD score ≥ 25.3 and/or a PhyloP score ≥ 7.367 were flagged (thresholds taken from Pejaver *et al*(30)). After filtering to only include variants with one or more of these variant annotations, we retained eleven candidate DNVs (0.8% of the initial 1,311 DNVs) each found in a different individual (Figure 1; Table 1).

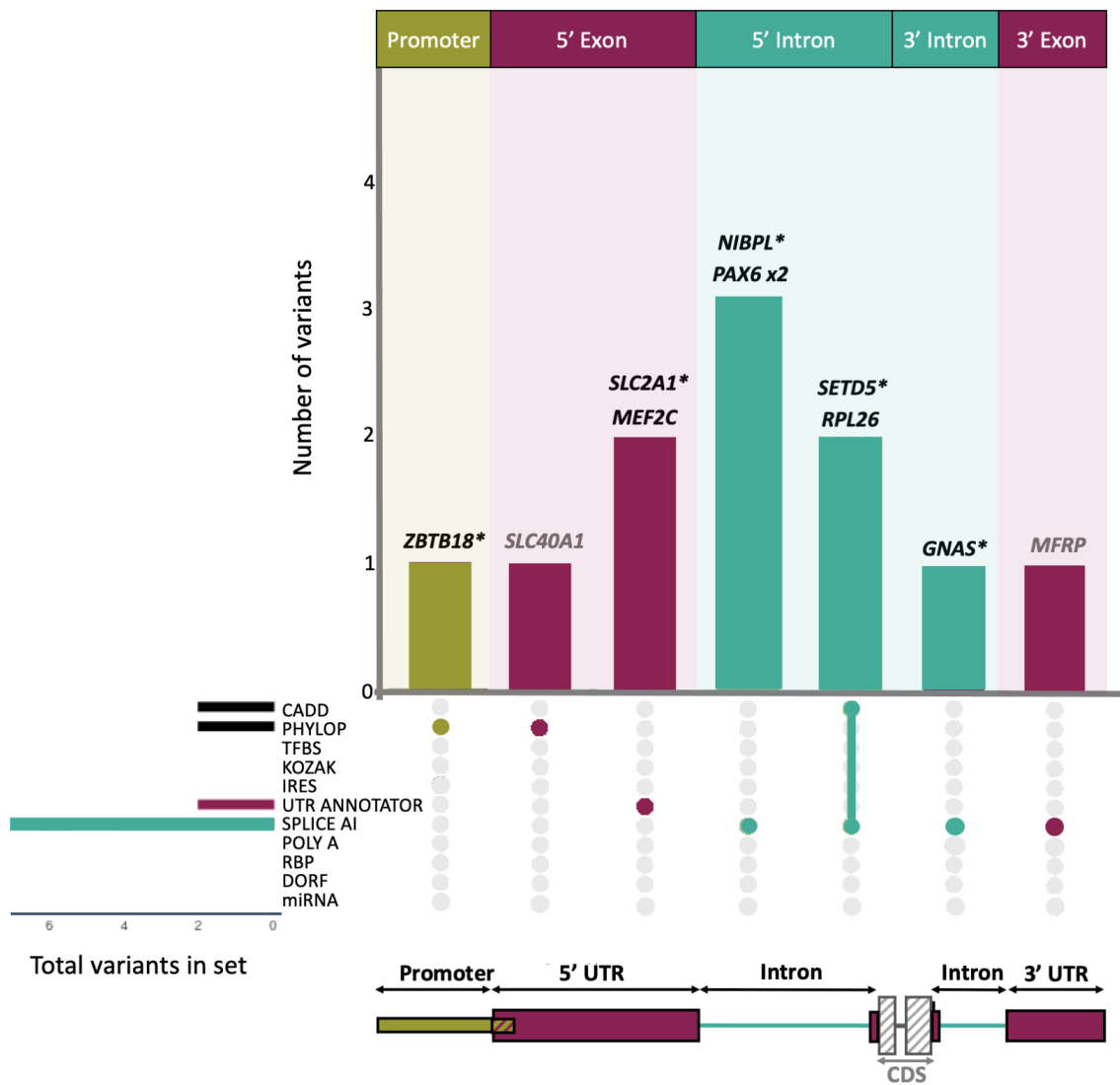


Figure 1: Prioritised *de novo* variants split by region and variant annotations. DNVs were identified from the Genomics England *de novo* dataset in the following regions: Promoter (mustard), UTR exons (raspberry), UTR/Promoter overlapping region (mustard and raspberry stripes), and UTR introns (teal). The gene names corresponding to identified DNVs are written above the corresponding bar. Those in black represent likely diagnoses (nine probands), with those in grey not being a good phenotypic match (two probands). Novel potential diagnoses are marked by an asterisk. Vertical bars in the top panel denote the number of variants identified with specific region and variant annotations that are represented by the bar colour (region annotations), and in the upset plot below (variant annotations). The total number of DNVs with each variant annotation is shown by the horizontal bars to the left of the upset.

Table 1: Details of prioritised *de novo* variants. Including the variant annotation which led to it being prioritised, the HPO terms associated with the patient, and whether or not this represents a likely diagnosis. Due to GEL policies, all HPO terms have been re-coded to parent terms with at least one level of abstraction (in some cases up to two) in order to protect the anonymity of participants. Inheritance: autosomal dominant (AD), autosomal recessive (AR), not specified (NS).

Variant (GRCh38)	Gene (transcript)	Known disease(s) linked to gene	Region annotation	Variant annotation details	Anonymised HPO terms	Possible diagnosis
Chr1:2440 51270 C>T	<i>ZBTB18</i> (ENST00000358704)	Intellectual Developmental Disorder, (AD; OMIM:612337)	Promoter	PhyloP = 7.426	Abnormality of higher mental function HP:0011446 Abnormality of speech or vocalisation HP:0002167 Motor delay HP:0001270	Yes
Chr1:4295 8758 C>T	<i>SLC2A1</i> (ENST00000426263)	Epilepsy, Idiopathic generalized, susceptibility to, 12, (AD; OMIM:614847), GLUT1 deficiency syndrome 1 (AD&AR; OMIM:606777) and 2	5'UTR	UTRannotator: uAUG gained. Out of frame oORF (c.-107G>A)	Abnormal nervous system physiology HP:0012638 Abnormal homeostasis HP:0012337 Phenotypic abnormality HP:0000118 Ataxia HP:0001251	Yes

		<p>GLUT1 deficiency syndrome 1, (AD OMIM:612126),</p> <p>Stomatin-deficient chryohydrocytosis with neurologic defects, (AD; OMIM:608885),</p> <p>Dystonia 9, (AD; OMIM: 601042)</p>			<p>Gait disturbance HP:0001288</p> <p>Neurodevelopmental delay HP:0012758</p>	
<p>Chr2:1895 80685 A>C</p>	<p><i>SLC40A1</i> (ENST00000261024)</p>	<p>Hemochromatosis, Type 4, (AD; OMIM:606069)</p>	<p>5'UTR</p>	<p>PhyloP = 8.189 (c.-225T>G)</p>	<p>Azotemia HP:0002157</p> <p>Abnormal hepatic glycogen storage HP:0500030</p> <p>Reduced consciousness/confusion HP:0004372</p> <p>Stroke HP:0001297</p> <p>Language impairment HP:0002463</p> <p>Hypertonia HP:0001276</p> <p>Phenotypic abnormality HP:0000118</p>	<p>No</p>
<p>Chr3:9397 978 G>A</p>	<p><i>SETD5</i> (ENST00000402198)</p>	<p>Intellectual developmental disorder, Autosomal Dominant, (AD; OMIM:615761)</p>	<p>5'UTR Splice</p>	<p>SpliceAI = 0.97 Donor loss (c.-177+1G>A)</p>	<p>Decreased body weight HP:0004325</p> <p>Abnormal facial shape HP:0001999</p> <p>Growth delay HP:0001510</p>	<p>Yes</p>

					<p>Aplasia/Hypoplasia of the mandible HP:0009118</p> <p>Intellectual disability HP:0001249</p> <p>Abnormal rib cage morphology HP:0001547</p> <p>Abnormal esophagus physiology HP:0025270</p> <p>Macrocephaly HP:0000256</p> <p>Abdominal symptom HP:0011458</p> <p>Asymmetric growth HP:0100555</p>	
Chr5:3695 3601 T>A	<i>NIBPL</i> (ENST00000282516)	Cornelia De Lange syndrome, (AD; OMIM:122470)	5'UTR Splice	SpliceAI = 0.24 Acceptor gain (c.-79-17T>A)	<p>Growth delay HP:0001510</p> <p>Abnormal upper lip morphology HP:0000177</p> <p>Abnormal digit morphology HP:0001167</p> <p>Neurodevelopmental abnormality HP:0012759</p> <p>Decreased head circumference</p>	Yes

					HP:0040195	
Chr5:8882 3814 G>A	<i>MEF2C</i> (ENST00000504921)	Neurodevelopmental disorder with hypotonia, stereotypic hand movements, and impaired language, (AD; OMIM:613443)	5'UTR	UTRannotator: uAUG gained. In frame oORF (c.-26C>T)	Abnormality of mouth size HP:0011337 Atypical behaviour HP:0000708 Neurodevelopmental abnormality HP:0012759 Motor delay HP:0001270 Reduced visual acuity HP:0007663 Decreased body weight HP:0004325 Neurodevelopmental delay HP:0012758 Aplasia/Hypoplasia of the corpus callosum HP:0007370 Abnormal nervous system physiology HP:0012638 Abnormal response to social norms HP:5200123 Abnormal eyelid morphology	Yes

					HP:0000492	
Chr11:318 06844 C>T	<i>PAX6</i> (ENST00000640368)	Aniridia 1, (AD), OMIM:106210. Foveal Hypoplasia 1, (AD; OMIM:136520), Anterior segment dysgenesis 5, (AD), (AD; OMIM:604229), Keratitis, Hereditary, (AD; OMIM:148190), Coloboma, ocular, autosomal dominant, (AD; OMIM:120200), Coloboma of optic nerve, (AD; OMIM:120430), Optic nerve hypoplasia, bilateral, (AD; OMIM:165550),	5'UTR Splice	SpliceAI = 0.56 Donor loss (c.-52+5G>A)	Phenotypic abnormality HP:0000118 Aplasia/Hypoplasia of the iris	Yes
Chr11:318 06926 CT>C	<i>PAX6</i> (ENST00000640368)	Aniridia 1, (AD), OMIM:106210. Foveal Hypoplasia 1, (AD; OMIM:136520), Anterior segment dysgenesis 5, (AD),	5'UTR Splice	SpliceAI = 0.65 Acceptor loss (c.-128-2del)	Aplasia/Hypoplasia of the iris	Yes

		(AD; OMIM:604229), Keratitis, Hereditary, (AD; OMIM:148190), Coloboma, ocular, autosomal dominant, (AD; OMIM:120200), Coloboma of optic nerve, (AD; OMIM:120430), Optic nerve hypoplasia, bilateral, (AD; OMIM:165550),				
Chr11:119 341418 C>A	<i>MFRP</i> (ENST00000619721)	Microphthalmia, isolated 5, (AR; OMIM:611040) Nanophthalmos 2, (NS; OMIM: 609549)	3'UTR	SpliceAI = 0.56 Donor gain (c.*130G>T)	Noncompaction cardiomyopathy Muscular ventricular septal defect HP:0011623 Abnormal cardiac septum morphology HP:0001671 Neurodevelopmental abnormality HP:0012759 Abnormal myocardium morphology HP:0001637	No

Chr17:838 2317 T>C	<i>RPL26</i> (ENST00000648839)	Diamond-Blackfan anemia 11, (AD; OMIM:614900)	5'UTR Splice	CADD_Phred = 35, SpliceAI = 0.97 Acceptor loss (c.-5-2A>G)	Periauricular skin pits HP:0100277 Radioulnar synostosis HP:0002974 Aplasia/Hypoplasia of the thumb HP:0009601 Abnormal zygomatic bone morphology HP:0010668 Thickened cortex of bones HP:0100039 Phenotypic abnormality HP:0000118 Abnormality of the musculoskeletal system HP:0033127 Slanting of the palpebral fissure HP:0200006 Atrial septal defect HP:0001631	Yes
Chr20:589 09654 A>G	<i>GNAS</i> (ENST00000371075)	Pseudohypoparathyroidism, Type IA, (AD; OMIM:103580) and 1B (AD; OMIM:603233), Pituitary adenoma 3, multiple types,	CDS/3' Intron	SpliceAI = 0.67 Acceptor gain (c.*625-30A>G)	Abnormality of the curvature of the cornea HP:0100691 Neurodevelopmental delay HP:0012758	Yes

		(NS; OMIM:617686), Pseudopseudohypoparathyroidism, (AD; OMIM:612463), Osseous heteroplasia, progressive, (AD; OMIM:166350), Pseudohypoparathyroidism, Type IC, (AD; OMIM:612462), McCune-Albright syndrome, (AD; OMIM:174800)			Hypothyroidism HP:0000821 Abnormality of body height HP:0000002 Phenotypic abnormality HP:0000118 Abnormality of refraction HP:0000539 Increased body weight HP:0004324	
--	--	---	--	--	--	--

Promoter and UTR DNVs provide a diagnosis for undiagnosed individuals with rare disease

Of the eleven remaining candidate variants, nine (82%) were assessed to be a good match for the individual's phenotype after detailed clinical review (see methods). Three of these had been flagged as diagnostic variants in GEL (in the 'exit questionnaire' table) prior to starting this work: two 5'UTR splicing variants in *PAX6* in two individuals with aniridia (OMIM:617141) and one 5'UTR splicing variant in *RPL26* in an individual with a previously undiagnosed monogenic disorder. A further variant, a 5'UTR variant that creates an upstream start codon in *MEF2C*, we previously identified as occurring *de novo* in three unrelated individuals with severe developmental disorders(2). Our approach successfully prioritised all rare DNVs within our candidate regions that had previously been identified as likely diagnostic in GEL. Together, these data demonstrate that our pipeline effectively identifies known diagnostic variants.

Four of the remaining five variants represent likely new diagnoses: (1) a 5'UTR uAUG-creating variant in *SLC2A1* in a patient with GLUT1 deficiency syndrome (OMIM:606777) that was not flagged by GEL as diagnostic, but that has been published previously(3) (Figure 2A). This uAUG is created into a strong start codon context and functional studies support its translation(3). Translation from this uAUG will prevent translation of the downstream CDS, leading to loss-of-function (Figure 2A). After returning this diagnosis to the recruiting clinical team it was classified as Likely Pathogenic and the individual is now on treatment; (2) A *NIPBL* splice disrupting (SpliceAI=0.24) variant 17 bp upstream of the final 5'UTR acceptor site in a participant with a phenotype closely related to Cornelia de Lange syndrome (OMIM:122470, Figure 2B). This variant introduces an AG dinucleotide which is predicted to result in a premature acceptor, however, the positioning of this within the 'AG exclusion zone' may also cause skipping of the exon containing the CDS start codon or other splice defects(60) (Figure 2B). The exact impact of this variant will need

to be confirmed through RNA studies, but RNA was not available for the patient; (3) A promoter variant that is located in a highly evolutionarily conserved position (PhyloP=7.426) 13 bp upstream of the TSS of *ZBTB18* in a participant with Intellectual disability; (4) A 5'UTR splice-site variant in *SETD5* in an individual originally suspected to have Silver Russell Syndrome (OMIM:180860). This variant is predicted to result in loss of the splice donor (SpliceAI=0.97) of the first 5'UTR exon at the canonical +1 position. DNA methylation signature analysis in this patient revealed an epismutation consistent with *SETD5-related neurodevelopmental disorder* (Figure 2C) and no other candidate variants were identified after screening the protein-coding regions of *SETD5*.

We also prioritised a cryptic splice variant in *GNAS* (SpliceAI=0.67) in a participant with hypothyroidism. Whilst we originally annotated this variant as within a 3'UTR intron for the MANE Plus Clinical transcript, the intron is between two CDS exons of the MANE Select transcript. Blood RNA-sequencing from the patient showed evidence of abnormal splicing of the MANE Select transcript, including intron retention (FRASER2 adjusted $P=1.67 \times 10^{-23}$), and significantly reduced expression (OUTRIDER adjusted $P=0.0019$; fold-change=0.66; Figure 2D), however the exact mechanism through which this variant could lead to disease is unclear.

For all candidate variants, we checked whether they were found in any other individuals across the full GEL cohort (i.e. not limiting to full trios or DNVs). Whilst we did not observe recurrence of any of the exact variants identified, we did identify a second participant with a different *SETD5* variant at the same genomic position (chr3:9397974 CAAGGT>C, hg38). On closer investigation, this variant is consistent with a germline *de novo*, but it fell just below the required coverage in one parent so it was excluded from the conservative high confidence *de novo* callset. DNA methylation signature analysis also confirmed *SETD5* as the diagnosis in this individual (Figure 2C). In total, we identified a likely disease-causing 'near-coding' DNV in ten of 8,040 individuals (0.0012%; nine initially prioritised variants and

one additional *SETD5* variant) who did not previously have a coding diagnosis. We classified all six newly identified variants as Likely Pathogenic following the ACMG/AMP guidelines (Supplementary Table 4)(8,61).

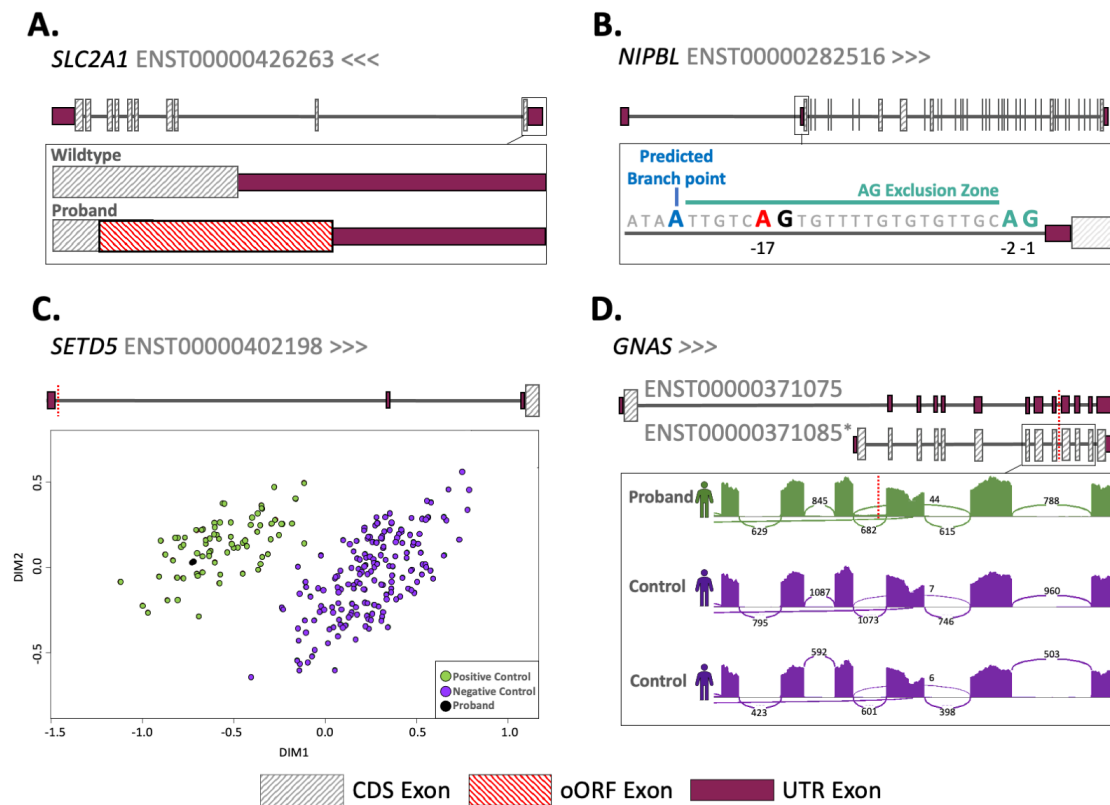
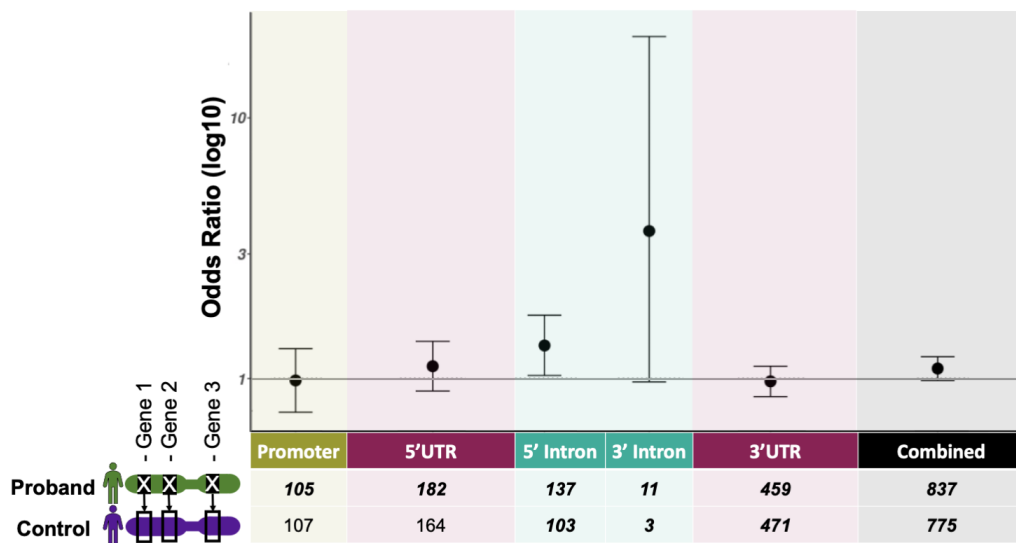


Figure 2: Candidate diagnostic *de novo* variants. A. Gene diagram showing the creation of an out of frame overlapping ORF (oORF; in red) in the *SLC2A1* gene in the proband. B. Illustration of the AG exclusion zone in the *NIPBL* gene. The T>A variant at the -17 position is marked in red, the most strongly predicted branch point (Branchpointer(62) 0.48), directly upstream of the AG exclusion zone is shown in blue. C. Multidimensional scaling plot showing differential methylation in *SETD5*. The position of both variants found in this gene are shown as red dotted lines. D. Sashimi plot showing aberrant splicing in the MANE Plus clinical transcript ENST00000371085. The proband shows some retention of the intron containing the variant (which is marked by a red dotted line) and increased skipping of the following exon compared to the controls (6.06X% vs 0.65X% and 1X%).

Burden testing does not detect a significant enrichment of variants with any collective region or variant annotation

Given we were able to identify disease-causing near-coding variants using our region-based filtering pipeline, we sought to further use this approach to quantify the enrichment of potentially damaging promoter and UTR variants. However, given the small number of trios within GEL with an unaffected child, and the fact that mutational models to directly assess enrichment of *de novo* variants (by comparing observed to expected numbers) have not been well calibrated for non-coding regions, specifically struggling with the 5' end of genes(63), we instead used the full aggregated set of inherited and *de novo* variants for our analysis. We matched each of 19,220 rare disease probands without a recorded protein-coding diagnosis, with replacement, to an unrelated unaffected individual from within the rare disease arm (unaffected parents) of GEL as a control on sex and genetically-inferred ancestry (see methods). The control individual was assigned the same dominant, green panelApp genes as had been assigned to the rare disease proband by GEL, allowing us to control for gene and region level differences in mutability (Figure 3). Given the disparity in panel size, with many probands having over 500 assigned green dominant genes (Supplementary Figure 2), to reduce noise we filtered probands to include only those to whom 100 or fewer green dominant PanelApp genes had been assigned (28% of all probands).

A.



B.

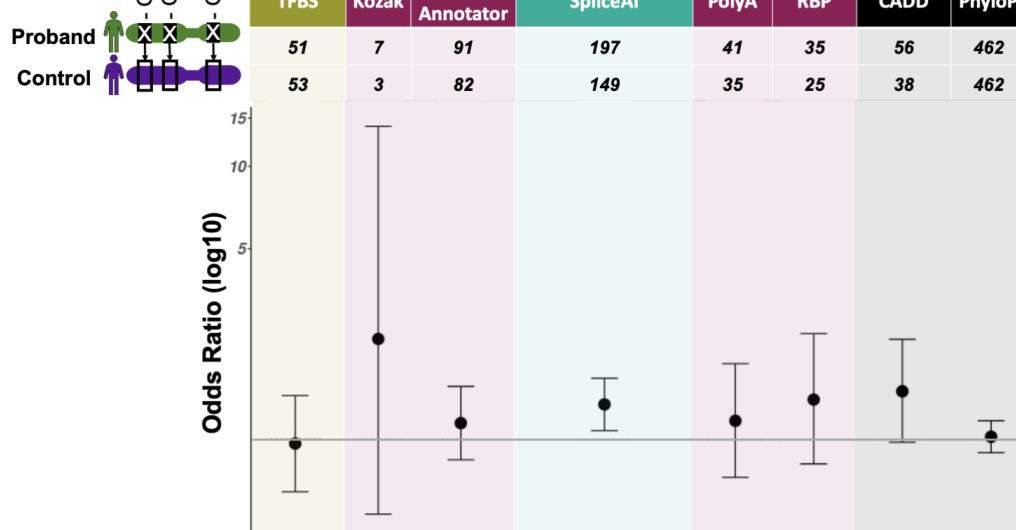


Figure 3: Burden testing results. Counts of variants and odd ratios (log10) testing for an enrichment of variants in cases compared to matched control participants (Fisher’s test), collectively by A. region annotation, and B. variant annotation. Annotation groups with fewer than 10 participants are omitted. Error bars represent 95% confidence intervals. Variants in 5’UTRs ($P=0.032$) and variants with SpliceAI ≥ 0.5 ($P=0.008$) are enriched in cases over matched controls, but neither is significant after correcting for multiple testing (Bonferroni threshold adjusting for 16 tests = 0.0031). Full results are in Supplementary Table 5.

After participant matching, we analysed a final set of 7,862 probands and 6,371 matched controls (1,295 matched controls were partnered with more than one proband). For all individuals, we extracted variants from GEL's aggregated variant dataset (AggV2) and filtered these using the same region-specific criteria applied to the *de novo* variants. Given that we used a high sensitivity SpliceAI threshold to prioritise DNVs with a high prior of pathogenicity, this was raised to a stricter cutoff of 0.5 for this analysis (Supplementary Figure 3). As we are not powered to analyse individual genes or gene-regions, we performed burden testing collectively across all prioritised variants with the same regional (e.g., 5'UTR) or variant-level (e.g. SpliceAI) annotations, across all participants and their assigned green genes. Whilst we observed a greater number of probands with prioritised variants compared with matched controls for the majority of regional and variant-level annotations we identified a greater number of probands with prioritised variants compared with matched controls, no specific annotation was significantly enriched for variants in cases after correcting for multiple testing (Figure 3; Supplementary Table 5). We also did not observe a significant enrichment when combining across all regions and variant annotations (Fisher's $P=0.109$, $OR=1.09$, 95% $CI=[0.981, 1.210]$).

Assuming a constant ratio between case and control variants, and hence ORs, we would need an estimated 11,610 cases and controls for significance at $P<0.05$ in the combined test across all region and variant annotations, and 26,066 for significance at a study-wide P -value threshold of <0.0031 , correcting for 16 tests (Supplementary Figure 4).

Discussion

Here, we have described a framework for the identification and annotation of potentially disease-causing UTR and promoter variants in individuals with rare disease. We show the

utility of the approach through identification of ten likely diagnoses in the GEL rare disease cohort. These comprised: three new confirmed diagnoses (*SLC2A1* and 2x *SETD5*) and three new likely diagnoses (*GNAS*, *NIPBL*, *ZBTB18*) alongside four previously confirmed diagnostic variants (2x *PAX6*, *RPL26*, and *MEF2C*). This illustrates the importance of expanding diagnostic screening into near coding regions of known disease genes.

In our analysis, we concentrated on variants within or directly adjacent to UTR exons and proximal promoter sequences for three key reasons: (1) the functional link between these regions and the impacted gene is relatively clear; (2) the importance of these regions in gene regulation means that variants within them can have a large impact, even causing complete loss-of-function; and (3) known functional elements within these regions enable us to predict some variant effects. Many of these criteria do not apply to more distal non-coding elements, such as enhancers, which also suffer from redundancy, meaning small variants in any one enhancer may often be unlikely to have a large impact on gene expression and hence disease(64), although there are exceptions(65). Recent work has, however, shown that variants impacting tissue-specific silencer elements may be a frequent cause of some disorders, indicating that these specific elements may have lower levels of redundancy(66,67). More research is needed to clarify the contribution of other non-coding elements to rare monogenic disorders.

A key barrier to routine identification of non-coding variants in clinical settings is the potential dramatic increase in interpretation burden. Here, we employed strict filters based on known regulatory mechanisms, aiming for high specificity. Consequently, a very large proportion of the shortlisted variants (~82%) were flagged as good diagnostic candidates following clinical review. This illustrates the validity of our method as a highly specific route to finding new diagnoses without dramatically increasing the number of variants that need to be manually reviewed. Here, we focus on *de novo* variants given their high prior probability of being pathogenic. Currently, *de novo* inheritance pattern, clinical fit, and functional validation are

essential to identifying and classifying non-coding variants as (likely) pathogenic. Hence it is much harder to identify disease-causing non-coding variants in more heterogeneous conditions and/or disorders where *de novo* variants are not a frequent disease mechanism. However, the same annotation approach can be applied to inherited variants(68).

Despite our strict filtering approach, the relatively modest number of new diagnoses given the size of the GEL cohort suggests that the proportion of currently undiagnosed individuals that will likely be diagnosed through regular assessment of proximal promoter and UTR regions will also be modest. This is in-line with the conclusions of our recent work looking for non-coding variants in recessive disease genes(68). Nevertheless, our diagnostic yield is likely an underestimate. First, we limited our analyses to only genes within a diagnostic panel applied to each individual and, within this we focussed on genes with a clear dominant disease mechanism. Gene agnostic approaches may have greater sensitivity for new diagnoses and allow the identification of candidate novel disease genes. Our study was also limited to MANE transcripts and may miss important variants impacting alternate transcripts. Our strict filtering approach was necessitated by our limited understanding of the 'regulatory genetic code', and the paucity of tools to accurately determine non-coding variant deleteriousness and also likely excluded some important variants. Finally, we only removed individuals flagged as 'solved' in the GEL 'exit questionnaire' as having an existing diagnosis. Many more individuals may have subsequently had likely diagnostic variants returned that were not reflected in the exit questionnaire at the time of analysis, due to ongoing analyses of the cohort.

Amongst our novel diagnoses was a 5'UTR uAUG-creating variant in *SLC2A1*, variants in which cause GLUT1 deficiency syndrome, which is treatable through diet. Hence, our diagnosis changed the clinical management of this patient. The exact same variant was found in a patient with a similar phenotype in 2017(3), the same year the patient was recruited to GEL, but, whilst the variant was deposited in the more specialist Leiden Open

Variation Database(69) (I.D: SLC2A1_000036) it did not appear in the more widely used ClinVar database until 2022 (ID:1491299). This highlights the necessity of data sharing through variant databases and the use of these datasets for re-analysis to reduce the lengthy diagnostic odysseys so often faced by individuals with rare disease.

Whilst we expected the excess burden of near-coding variants in cases to be relatively low, our approach was imperfect. In particular, analysing all variants identified in each individual (i.e., inherited as well as *de novo*) across large gene panels likely added a lot of noise. A better approach to assess this enrichment would be using only *de novo* variants, however, the number of trios within GEL where the child is unaffected is very small, and we and others have struggled to correctly optimise mutational models for application at the 5' end of genes(63). Multiple additional factors also likely contribute to our observed lack of signal. Firstly, we used unaffected parents of rare disease probands as a control and these individuals may be more likely to carry damaging variants (for example variants with reduced penetrance, or variants that modify coding variant penetrance). Secondly, the sizes of gene panels varied substantially between participants, with some containing vast numbers of genes (Supplementary Figure 2). These larger panels likely contribute an overrepresentation of variants that are unlikely to be causal.

Conclusions

Our understanding of the mechanisms that underlie variation in the non-coding genome is far from complete. Despite this, routine interrogation of these regions with existing knowledge and tools can return valuable genetic diagnoses to patients. Identifying more disease-causing variants in non-coding regions and understanding how they lead to disease will, in turn, increase our understanding of regulatory biology, and enable us to create better tools to identify and annotate these variants. Here, focussing specifically on proximal promoters, UTRs, and UTR introns, we developed a flexible approach for variant annotation

and filtering which can be extended and adapted to incorporate new functional variant classes as our understanding of non-coding genome biology increases. Our framework provides a foundation for the systematic analysis of variants in these regions, which can be readily applied to cohorts, and in clinical settings, globally.

Acknowledgements

NWhiffin and ACM-G are supported by a Sir Henry Dale Fellowship awarded to NWhiffin, jointly funded by the Wellcome Trust and the Royal Society (220134/Z/20/Z). NW, END, and MF are supported by research grant funding from the Rosetrees Trust (PGL19-2/10025). AJMB is supported by a Wellcome PhD Training Fellowship for Clinicians and the 4Ward North PhD Programme for Health Professionals (223521/Z/21/Z). JL is supported by a University of Southampton Anniversary Fellowship. DB is supported by a National Institute for Health Research (NIHR) (RP-2016-07-011) research professorship. SJS is supported by grant funding from the National Institutes of Health (NIH) (R01 MH116999 S.J.S. and U01 MH122681)

This research was made possible through access to data in the National Genomic Research Library, which is managed by Genomics England Limited (a wholly owned company of the Department of Health and Social Care). The National Genomic Research Library holds data provided by patients and collected by the NHS as part of their care and data collected as part of their participation in research. The National Genomic Research Library is funded by the National Institute for Health Research and NHS England. The Wellcome Trust, Cancer Research UK and the Medical Research Council have also funded research infrastructure.

We would like to acknowledge the Genomics England service desk, in particular Daniel Rhodes, Roel Bevers, and Peter O'Donovan, for the support and guidance they provided to

make this work possible. We would also like to thank Ana Lisa Taylor Tavares for her assistance in orchestrating connections with clinical collaborators, and both Esther Ng and Matteo Ferla for valuable discussions, and insight.

We acknowledge Episign® for the diagnostic DNA methylation array testing, and are grateful for the support of the NIHR Manchester Biomedical Research Centre (NIHR203308).

References

1. Blakes AJM, Wai HA, Davies I, Moledina HE, Ruiz A, Thomas T, et al. A systematic analysis of splicing variants identifies new diagnoses in the 100,000 Genomes Project. *Genome Med.* 2022 Jul 26;14(1):1–11.
2. Wright CF, Quaife NM, Ramos-Hernández L, Danecek P, Ferla MP, Samocha KE, et al. Non-coding region variants upstream of MEF2C cause severe developmental disorder through three distinct loss-of-function mechanisms. *Am J Hum Genet.* 2021 Jun 3;108(6):1083–94.
3. Willemsen MA, Vissers LE, Verbeek MM, van Bon BW, Geuer S, Gilissen C, et al. Upstream SLC2A1 translation initiation causes GLUT1 deficiency syndrome. *Eur J Hum Genet.* 2017 Jun;25(6):771–4.
4. Kircher M, Xiong C, Martin B, Schubach M, Inoue F, Bell RJA, et al. Saturation mutagenesis of twenty disease-associated regulatory elements at single base-pair resolution. *Nat Commun [Internet].* 2019 Aug 8 [cited 2023 Sep 12];10(1). Available from: <https://pubmed.ncbi.nlm.nih.gov/31395865/>
5. Griesemer D, Xue JR, Reilly SK, Ulirsch JC, Kukreja K, Davis JR, et al. Genome-wide functional screen of 3'UTR variants uncovers causal variants for human disease and evolution. *Cell [Internet].* 2021 Sep 30 [cited 2023 Sep 12];184(20). Available from: <https://pubmed.ncbi.nlm.nih.gov/34534445/>
6. Das S, Vera M, Gandin V, Singer RH, Tutucci E. Intracellular mRNA transport and localized translation. *Nat Rev Mol Cell Biol.* 2021 Apr 9;22(7):483–504.
7. Sonneveld S, Verhagen BMP, Tanenbaum ME. Heterogeneity in mRNA Translation. *Trends Cell Biol.* 2020 Aug 1;30(8):606–18.
8. Ellingford JM, Ahn JW, Bagnall RD, Baralle D, Barton S, Campbell C, et al. Recommendations for clinical interpretation of variants found in non-coding regions of the genome. *Genome Med.* 2022 Jul 19;14(1):1–19.
9. Whiffin N, Karczewski KJ, Zhang X, Chothani S, Smith MJ, Evans DG, et al. Characterising the loss-of-function impact of 5' untranslated region variants in 15,708 individuals. *Nat Commun.* 2020 May 27;11(1):1–12.
10. Mohan RA, van Engelen K, Stefanovic S, Barnett P, Ilgun A, Baars MJ, et al. A mutation in the Kozak sequence of GATA4 hampers translation in a family with atrial septal defects. *Am J Med Genet A [Internet].* 2014 Nov [cited 2023 May 10];164A(11). Available from: <https://pubmed.ncbi.nlm.nih.gov/25099673/>
11. Filatova AY, Vasilyeva TA, Marakhonov AV, Sukhanova NV, Voskresenskaya AA, Zinchenko RA, et al. Upstream ORF frameshift variants in the PAX6 5'UTR cause congenital aniridia. *Hum Mutat.* 2021 Aug 1;42(8):1053–65.
12. Curinha A, Braz SO, Pereira-Castro I, Cruz A, Moreira A. Implications of polyadenylation in health and disease. *Nucleus [Internet].* 2015 Jan 6 [cited 2023 May 10]; Available from: <https://www.tandfonline.com/doi/abs/10.4161/nucl.36360>

13. Rey AD, del Pozo Valero M, Bouckaert M, Van Den Broeck F, Varela MD, Van Heetvelde M, et al. Combining a prioritization strategy and functional studies nominates 5'UTR variants underlying inherited retinal disease [Internet]. medRxiv. 2023 [cited 2023 Jul 26]. p. 2023.06.19.23291376. Available from: <https://www.medrxiv.org/content/10.1101/2023.06.19.23291376v1.abstract>
14. Gutierrez-Rodrigues F, Donaires FS, Pinto A, Vicente A, Dillon LW, Clé DV, et al. Pathogenic TERT promoter variants in telomere diseases. *Genet Med*. 2018 Dec 7;21(7):1594–602.
15. Villicaña S, Bell JT. Genetic impacts on DNA methylation: research findings and future perspectives. *Genome Biol*. 2021 Apr 30;22(1):1–35.
16. Montulli L, Grobe M, Rezac C. Lynx web browser [Internet]. 1992 [cited 2023 May 18]. Available from: https://lynx.invisible-island.net/lynx_help/Lynx_users_guide.html
17. Morales J, Pujar S, Loveland JE, Astashyn A, Bennett R, Berry A, et al. A joint NCBI and EMBL-EBI transcript set for clinical genomics and research. *Nature*. 2022 Apr;604(7905):310–5.
18. Moore JE, Purcaro MJ, Pratt HE, Epstein CB, Shores N, Adrian J, et al. Expanded encyclopaedias of DNA elements in the human and mouse genomes. *Nature*. 2020 Jul 29;583(7818):699–710.
19. Quinlan AR, Hall IM. BEDTools: a flexible suite of utilities for comparing genomic features. *Bioinformatics*. 2010 Jan 28;26(6):841–2.
20. De novo variant research dataset - Genomics England Trusted Research Environment User Guide [Internet]. [cited 2023 Jul 19]. Available from: https://re-docs.genomicsengland.co.uk/de_novo_data/
21. Genomics England. Labkey API - Genomics England Research Environment User Guide [Internet]. 2023 [cited 2023 May 10]. Available from: https://re-docs.genomicsengland.co.uk/labkey_api/
22. De novo variant research dataset - Genomics England Trusted Research Environment User Guide [Internet]. [cited 2023 Jul 27]. Available from: https://re-docs.genomicsengland.co.uk/de_novo_data/
23. Genomics England. Principal Components and genetically inferred relatedness - Genomics England Research Environment User Guide [Internet]. 2023 [cited 2023 May 10]. Available from: https://re-docs.genomicsengland.co.uk/principal_components/
24. Kuhn RM, Haussler D, Kent WJ. The UCSC genome browser and associated tools. *Brief Bioinform*. 2013 Mar;14(2):144–61.
25. McLaren W, Gil L, Hunt SE, Riat HS, Ritchie GRS, Thormann A, et al. The Ensembl Variant Effect Predictor. *Genome Biol*. 2016 Jun 6;17(1):122.
26. Rentzsch P, Schubach M, Shendure J, Kircher M. CADD-Splice-improving genome-wide variant effect prediction using deep learning-derived splice scores. *Genome Med*. 2021 Feb 22;13(1):31.
27. Pollard KS, Hubisz MJ, Rosenbloom KR, Siepel A. Detection of nonneutral substitution rates on mammalian phylogenies. *Genome Res*. 2010 Jan;20(1):110–21.
28. Landrum MJ, Chitipiralla S, Brown GR, Chen C, Gu B, Hart J, et al. ClinVar: improvements to accessing data. *Nucleic Acids Res*. 2020 Jan 8;48(D1):D835–44.
29. Zhang X, Wakeling M, Ware J, Whiffin N. Annotating high-impact 5'untranslated region variants with the UTRannotator. *Bioinformatics*. 2021 May 23;37(8):1171–3.
30. Pejaver V, Byrne AB, Feng BJ, Pagel KA, Mooney SD, Karchin R, et al. Calibration of computational tools for missense variant pathogenicity classification and ClinGen recommendations for PP3/BP4 criteria. *Am J Hum Genet*. 2022 Dec 1;109(12):2163–77.
31. Zhao J, Li Y, Wang C, Zhang H, Zhang H, Jiang B, et al. IRESbase: A Comprehensive Database of Experimentally Validated Internal Ribosome Entry Sites. *Genomics Proteomics Bioinformatics*. 2020 Apr;18(2):129–39.
32. Plotnikova O, Baranova A, Skoblov M. Comprehensive Analysis of Human microRNA–mRNA Interactome. *Front Genet* [Internet]. 2019 Oct 8 [cited 2023 May 26];10. Available from: <http://dx.doi.org/10.3389/fgene.2019.00933>
33. Nowakowski TJ, Rani N, Golkaram M, Zhou HR, Alvarado B, Huch K, et al. Regulation of cell-type-specific transcriptomes by microRNA networks during human brain development. *Nat Neurosci*. 2018 Nov 19;21(12):1784–92.

34. Spengler RM, Zhang X, Cheng C, McLendon JM, Skeie JM, Johnson FL, et al. Elucidation of transcriptome-wide microRNA binding sites in human cardiac tissues by Ago2 HITS-CLIP. *Nucleic Acids Res.* 2016 Jul 14;44(15):7120–31.
35. Boudreau RL, Jiang P, Gilmore BL, Spengler RM, Tirabassi R, Nelson JA, et al. Transcriptome-wide Discovery of microRNA Binding Sites in Human Brain. *Neuron.* 2014 Jan 22;81(2):294–305.
36. Chothani SP, Adami E, Widjaja AA, Langley SR, Viswanathan S, Pua CJ, et al. A high-resolution map of human RNA translation. *Mol Cell.* 2022 Aug 4;82(15):2885–99.e8.
37. Pisarev AV, Kolupaeva VG, Pisareva VP, Merrick WC, Hellen CUT, Pestova TV. Specific functional interactions of nucleotides at key -3 and +4 positions flanking the initiation codon with components of the mammalian 48S translation initiation complex. *Genes Dev.* 2006 Mar 1;20(5):624–36.
38. Findlay SD, Romo L, Burge CB. Quantifying negative selection in human 3' UTRs uncovers constrained targets of RNA-binding proteins [Internet]. *bioRxiv.* 2022 [cited 2023 May 16]. p. 2022.11.30.518628. Available from: <https://www.biorxiv.org/content/10.1101/2022.11.30.518628v1.abstract>
39. Jens M, McGurk M, Bundschuh R, Burge CB. RBPamp: Quantitative Modeling of Protein-RNA Interactions in vitro Predicts in vivo Binding [Internet]. *bioRxiv.* 2022 [cited 2023 Jul 27]. p. 2022.11.08.515616. Available from: <https://www.biorxiv.org/content/10.1101/2022.11.08.515616v1.abstract>
40. Ren F, Zhang N, Zhang L, Miller E, Pu JJ. Alternative Polyadenylation: a new frontier in post transcriptional regulation. *Biomarker Research.* 2020 Nov 25;8(1):1–10.
41. Vierstra J, Lazar J, Sandstrom R, Halow J, Lee K, Bates D, et al. Global reference mapping of human transcription factor footprints. *Nature.* 2020 Jul;583(7818):729–36.
42. Steinhaus R, Robinson PN, Seelow D. FABIAN-variant: predicting the effects of DNA variants on transcription factor binding. *Nucleic Acids Res.* 2022 May 26;50(W1):W322–9.
43. Mathelier A, Wasserman WW. The next generation of transcription factor binding site prediction. *PLoS Comput Biol.* 2013 Sep 5;9(9):e1003214.
44. Genomics England. Ancestry inference - Genomics England Research Environment User Guide [Internet]. 2023 [cited 2023 May 10]. Available from: https://re-docs.genomicsengland.co.uk/ancestry_inference/
45. Aggregated variant calls - genomics England research environment user guide [Internet]. [cited 2023 May 15]. Available from: <https://re-docs.genomicsengland.co.uk/aggv2/>
46. Pedersen BS, Brown JM, Dashnow H, Wallace AD, Velinder M, Tristani-Firouzi M, et al. Effective variant filtering and expected candidate variant yield in studies of rare human disease. *NPJ Genom Med.* 2021 Jul 15;6(1):60.
47. Manichaikul A, Mychaleckyj JC, Rich SS, Daly K, Sale M, Chen WM. Robust relationship inference in genome-wide association studies. *Bioinformatics.* 2010 Oct 5;26(22):2867–73.
48. Robinson JT, Thorvaldsdóttir H, Winckler W, Guttman M, Lander ES, Getz G, et al. Integrative genomics viewer. *Nat Biotechnol.* 2011 Jan 1;29(1):24–6.
49. Scheller IF, Lutz K, Mertes C, Yépez VA, Gagneur J. Improved detection of aberrant splicing using the Intron Jaccard Index [Internet]. *medRxiv.* 2023 [cited 2023 Aug 21]. p. 2023.03.31.23287997. Available from: <https://www.medrxiv.org/content/10.1101/2023.03.31.23287997v1.abstract>
50. OUTRIDER: A Statistical Method for Detecting Aberrantly Expressed Genes in RNA Sequencing Data. *Am J Hum Genet.* 2018 Dec 6;103(6):907–17.
51. Levy MA, McConkey H, Kerkhof J, Barat-Houari M, Bargiacchi S, Biamino E, et al. Novel diagnostic DNA methylation epigenatures expand and refine the epigenetic landscapes of Mendelian disorders. *HGG advances* [Internet]. 2021 Dec 3 [cited 2023 Sep 7];3(1). Available from: <https://pubmed.ncbi.nlm.nih.gov/35047860/>
52. Barili V, Ambrosini E, Uliana V, Bellini M, Vitetta G, Martorana D, et al. Success and Pitfalls of Genetic Testing in Undiagnosed Diseases: Whole Exome Sequencing and Beyond. *Genes* [Internet]. 2023 Jun 10 [cited 2023 Sep 7];14(6). Available from: <https://pubmed.ncbi.nlm.nih.gov/37372421/>
53. The R Project for Statistical Computing [Internet]. [cited 2023 Aug 22]. Available from: <https://www.R-project.org/>
54. A Grammar of Data Manipulation [R package dplyr version 1.1.2]. 2023 Apr 20 [cited 2023 Aug 22];

Available from: <https://CRAN.R-project.org/package=dplyr>

55. Tidy Messy Data [R package tidyr version 1.3.0]. 2023 Jan 24 [cited 2023 Aug 22]; Available from: <https://CRAN.R-project.org/package=tidyr>
56. Wickham H. Simple, Consistent Wrappers for Common String Operations [R package stringr version 1.5.0]. 2022 Dec 2 [cited 2023 Aug 22]; Available from: <https://CRAN.R-project.org/package=stringr>
57. Conway JR, Lex A, Gehlenborg N. UpSetR: an R package for the visualization of intersecting sets and their properties. *Bioinformatics*. 2017 Sep 15;33(18):2938–40.
58. Create Elegant Data Visualisations Using the Grammar of Graphics [R package ggplot2 version 3.4.3]. 2023 Aug 14 [cited 2023 Aug 22]; Available from: <https://CRAN.R-project.org/package=ggplot2>
59. Martin AR, Williams E, Foulger RE, Leigh S, Daugherty LC, Niblock O, et al. PanelApp crowdsources expert knowledge to establish consensus diagnostic gene panels. *Nat Genet*. 2019 Nov 1;51(11):1560–5.
60. Bryen SJ, Yuen M, Joshi H, Dawes R, Zhang K, Lu JK, et al. Prevalence, parameters, and pathogenic mechanisms for splice-altering acceptor variants that disrupt the AG exclusion zone. *Human Genetics and Genomics Advances* [Internet]. 2022 Oct 10 [cited 2023 Jul 26];3(4). Available from: <https://www.ncbi.nlm.nih.gov/pmc/articles/PMC9284458/>
61. Richards S, Aziz N, Bale S, Bick D, Das S, Gastier-Foster J, et al. Standards and Guidelines for the Interpretation of Sequence Variants: A Joint Consensus Recommendation of the American College of Medical Genetics and Genomics and the Association for Molecular Pathology. *Genet Med*. 2015 May;17(5):405.
62. Signal B, Gloss BS, Dinger ME, Mercer TR. Machine-learning annotation of human splicing branchpoints [Internet]. *bioRxiv*. 2016 [cited 2023 Aug 11]. p. 094003. Available from: <https://www.biorxiv.org/content/10.1101/094003v1.abstract>
63. Chen S, Francioli LC, Goodrich JK, Collins RL, Kanai M, Wang Q, et al. A genome-wide mutational constraint map quantified from variation in 76,156 human genomes [Internet]. *bioRxiv*. 2022 [cited 2023 Jul 26]. p. 2022.03.20.485034. Available from: <https://www.biorxiv.org/content/10.1101/2022.03.20.485034v2.abstract>
64. Kvon EZ, Waymack R, Gad M, Wunderlich Z. Enhancer redundancy in development and disease. *Nat Rev Genet* [Internet]. 2021 May [cited 2023 Aug 15];22(5). Available from: <https://pubmed.ncbi.nlm.nih.gov/33442000/>
65. Fantauzzo KA, Tadin-Strapps M, You Y, Mentzer SE, Baumeister FAM, Cianfarani S, et al. A position effect on TRPS1 is associated with Ambras syndrome in humans and the Koala phenotype in mice. *Hum Mol Genet*. 2008 Aug 19;17(22):3539–51.
66. Tenney AP, Di Gioia SA, Webb BD, Chan WM, de Boer E, Garnai SJ, et al. Noncoding variants alter GATA2 expression in rhombomere 4 motor neurons and cause dominant hereditary congenital facial paresis. *Nat Genet*. 2023 Jun 29;55(7):1149–63.
67. Wakeling MN, Owens NDL, Hopkinson JR, Johnson MB, Houghton JAL, Dastamani A, et al. Non-coding variants disrupting a tissue-specific regulatory element in HK1 cause congenital hyperinsulinism. *Nat Genet* [Internet]. 2022 Nov [cited 2023 Jul 26];54(11). Available from: <https://pubmed.ncbi.nlm.nih.gov/36333503/>
68. Lord J, Oquendo CJ, Martin-Geary A, Blakes AJM, Arciero E, Domcke S, et al. Non-coding variants are a rare cause of recessive developmental disorders in trans with coding variants [Internet]. *medRxiv*. 2023 [cited 2023 Jul 19]. p. 2023.06.23.23291805. Available from: <https://www.medrxiv.org/content/10.1101/2023.06.23.23291805v1.abstract>
69. Fokkema IFA, Taschner PEM, Schaafsma GCP, Celli J, Laros JFJ, den Dunnen JT. LOVD v.2.0: the next generation in gene variant databases. *Hum Mutat*. 2011 May 1;32(5):557–63.